Return to previous file: MCU9.pdf

Table 2: Tidal harmonic analysis of the *east-west* component of the depth-averaged (1-metre depth bins 1-19) current at the offshore site.

Tide name	Frequency (hrs)	Amplitude ($m\ s^{-1}$)	Amplitude error ($m\ s^{-1}$)	Phase (°NZST)	Phase error (°NZST)
*MM	0.00151	0.0064	0.021	53.55	190.85
*MSF	0.00282	0.0011	0.021	159.62	1092.67
*ALP1	0.03440	0.0069	0.006	132.32	44.38
*2Q1	0.03571	0.0058	0.006	190.98	52.46
*Q1	0.03722	0.0036	0.006	156.07	84.93
*O1	0.03873	0.0209	0.006	200.50	14.94
*NO1	0.04027	0.0058	0.006	172.28	53.95
*K1	0.04178	0.0312	0.006	236.62	10.45
*J1	0.04329	0.0023	0.006	66.17	129.12
*OO1	0.04483	0.0042	0.006	22.56	56.07
*UPS1	0.04634	0.0009	0.006	298.25	257.14
*EPS2	0.07618	0.0033	0.004	235.94	61.93
*MU2	0.07769	0.0015	0.004	72.17	139.87
*N2	0.07900	0.0057	0.004	136.58	37.77
*M2	0.08051	0.0146	0.004	181.78	14.58
*L2	0.08202	0.0041	0.004	216.88	48.95
*S2	0.08333	0.0018	0.004	141.30	115.95
*ETA2	0.08507	0.0016	0.004	339.96	90.86
*MO3	0.11924	0.0015	0.003	176.01	92.18
*M3	0.12077	0.0013	0.003	324.23	114.97
*MK3	0.12229	0.0026	0.003	299.56	54.98
*SK3	0.12511	0.0004	0.003	254.51	334.37
*MN4	0.15951	0.0005	0.002	307.00	199.89
*M4	0.16102	0.0027	0.002	327.65	39.63
*SN4	0.16233	0.0018	0.002	242.43	58.63
*MS4	0.16384	0.0019	0.002	174.42	55.52
*S4	0.16667	0.0009	0.002	147.47	111.70
*2MK5	0.20280	0.0005	0.001	55.74	153.69
*2SK5	0.20845	0.0010	0.001	274.58	64.42
*2MN6	0.24002	0.0005	0.001	205.19	109.05
*M6	0.24153	0.0010	0.001	3.67	55.86
*2MS6	0.24436	0.0003	0.001	92.60	196.06
*2SM6	0.24718	0.0015	0.001	298.44	35.81
*3MK7	0.28331	0.0002	0.001	267.52	272.92

Table 3: Tidal harmonic analysis of the *north-south* component of the depth-averaged (1-metre depth bins 1-19) current at the offshore site.

Tide name	Frequency (hrs)	Amplitude ($m\ s^{-1}$)	Amplitude error ($m\ s^{-1}$)	Phase (°NZST)	Phase error (°NZST)
*MM	0.00151	0.0081	0.019	334.18	133.97
*MSF	0.00282	0.0095	0.019	140.85	113.15
*ALP1	0.03440	0.0073	0.004	127.28	28.09
*2Q1	0.03571	0.0062	0.004	195.96	32.68
*Q1	0.03722	0.0077	0.004	130.69	26.63
*O1	0.03873	0.0305	0.004	193.31	6.80
*NO1	0.04027	0.0061	0.004	163.45	33.89
*K1	0.04178	0.0314	0.004	238.07	6.90
*J1	0.04329	0.0011	0.004	113.02	176.78
*OO1	0.04483	0.0044	0.004	36.07	35.67
*UPS1	0.04634	0.0012	0.004	1.61	125.00
*EPS2	0.07618	0.0008	0.002	310.43	177.43
*MU2	0.07769	0.0042	0.002	32.60	33.70
*N2	0.07900	0.0058	0.002	101.09	25.09
*M2	0.08051	0.0314	0.002	116.14	4.59
*L2	0.08202	0.0064	0.002	209.80	21.13
*S2	0.08333	0.0042	0.002	189.09	33.59
*ETA2	0.08507	0.0015	0.002	2.03	65.68
*MO3	0.11924	0.0009	0.002	228.41	91.85
*M3	0.12077	0.0018	0.002	169.96	51.56
*MK3	0.12229	0.0007	0.002	172.97	129.58
*SK3	0.12511	0.0016	0.002	100.01	52.45
*MN4	0.15951	0.0017	0.001	215.78	37.85
*M4	0.16102	0.0018	0.001	154.72	34.23
*SN4	0.16233	0.0012	0.001	200.72	49.93
*MS4	0.16384	0.0008	0.001	275.33	73.54
*S4	0.16667	0.0014	0.001	227.07	41.89
*2MK5	0.20280	0.0006	0.001	337.10	99.90
*2SK5	0.20845	0.0012	0.001	278.57	47.12
*2MN6	0.24002	0.0013	0.001	269.87	35.76
*M6	0.24153	0.0006	0.001	266.82	77.02
*2MS6	0.24436	0.0002	0.001	281.97	293.51
*2SM6	0.24718	0.0004	0.001	294.02	119.80
*3MK7	0.28331	0.0004	0.001	273.77	99.67

3.3 Non-tidal currents

Using data from the tidal harmonic analysis, the tidal current accounted for 36% and 16% of the total current variance at the offshore and inshore sites respectively. Currents driven by local winds (e.g., Gisborne airport) account for some of the non-tidal variance. This is demonstrated by a wavelet analysis of the wind and current time-series (e.g., Figure 10).

Wavelet analysis is a comparatively recent tool designed to resolve the dominant modes of variability (periodic oscillations) of a time-series and how those modes vary with time (Torrence & Compo 1998). It is specifically designed to deal with non-stationary signals that vary with time and is therefore ideally suited to identifying correlations between wind and wind-driven currents. Continuous wavelets transforms were calculated following Torrence & Compo (1998) using a 32-parameter derivative-of-a-gaussian real-valued wavelet function, chosen to resolve seiche motion to a fine-scale in both time and frequency. Wavelet software was provided by C. Torrence and G. Compo, and is available at URL: http://paos.colorado.edu/research/wavelets.

Figure 10 is shown as an example to demonstrate that there were identifiable links between the wind and current time-series. The plot shows a wind-current cross-power contour map, which is a plot of the covariance between wind and current. The bright patches represent high power (greater than the 95% significance level) and the dark patches represent low (insignificant) power.

There are coherent fluctuations in the east-west component of both the wind and current time-series throughout the deployment, at periods of 24-hr (y-axis). The coherence demonstrates that the wind is transferring energy to the water column. The 24-hr oscillation period is most likely related to diurnal wind fluctuations, as winds blow offshore in the morning and onshore as the afternoon sea-breeze develops. There are other coherent "events" that occur at various modal periods at different times during the deployment (e.g., weather cycles 80-100 hrs between 16-26 Sep), demonstrating that wind transfers energy to the water column in a complex manner at varying time scales.

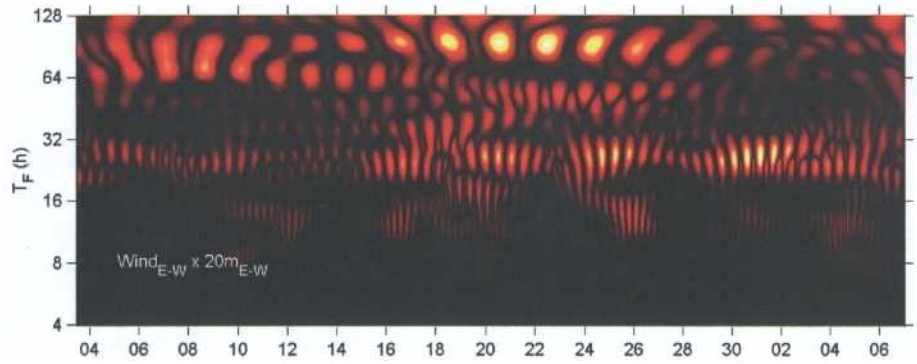

Figure 10: Cross-power (covariance) contour map of the square of the wavelet coefficients, calculated between the east-west components of the wind and current 20.5 m above the seabed at the offshore site. The bright patches represent high power (greater than the 95% significance level) and the dark patches represent low (insignificant) power. The x-axis is time as dates during Sep-Oct 2003, while the logarithmic y-axis is equivalent Fourier period or the modal period, in hours.

Cumulative vector plots show a theoretical particle travel path based on the current velocities measured at a single point. At the inshore site, the trend was for near-surface currents to flow offshore, while near-bed currents were significantly smaller with no clear trend, apart from early in the deployment when it followed the same offshore direction as the upper water column. Since tides tend to oscillate back and forth resulting in near-zero net drift, the near-surface drift at the inshore site appears to be forced by the generally offshore wind observed during the deployment (Figure 2).

At the offshore site, currents tended to consistently flow alongshore to the northeast, at all depths. This too, is in keeping with a wind-driven current, deflected to the left by the Coriolis force to produce an Ekman current (e.g., Pond & Pickard 1983). Being bounded by the coast the Ekman current would quickly become geostrophically balanced, and the results suggest that this part of the coast may be dominated by an inshore northward flowing wind-induced geostrophic current. Support is provided by the results of Stephens et al. (2001), who identified a similar northward flow 6 km offshore from the entrance to Poverty Bay during a deployment in September-October 1998, and Bell (1985) who recorded a net north-easterly flow at the entrance to Poverty Bay. The measurements of Chiswell and Roemmich (1998) and Chiswell (2000) showed an inshore coastal current flowing northward in the vicinity and to the north of the marine reserve area. Chiswell and Roemmich (1998) hinted this could be an inshore counter-current to the southward flowing East Cape current. From subsequent measurements Chiswell (2000) documented the Wairarapa Coastal Current that flows northward up the coast as far as Mahia Peninsula, but could possibly extend

further north at times. The northward flow appears to be a persistent feature on this part of the coast, regardless whether it forms part of the Wairarapa Coastal Current, as a counter-current to the East Cape Current further offshore, or is formed or modified by the prevailing regional wind.

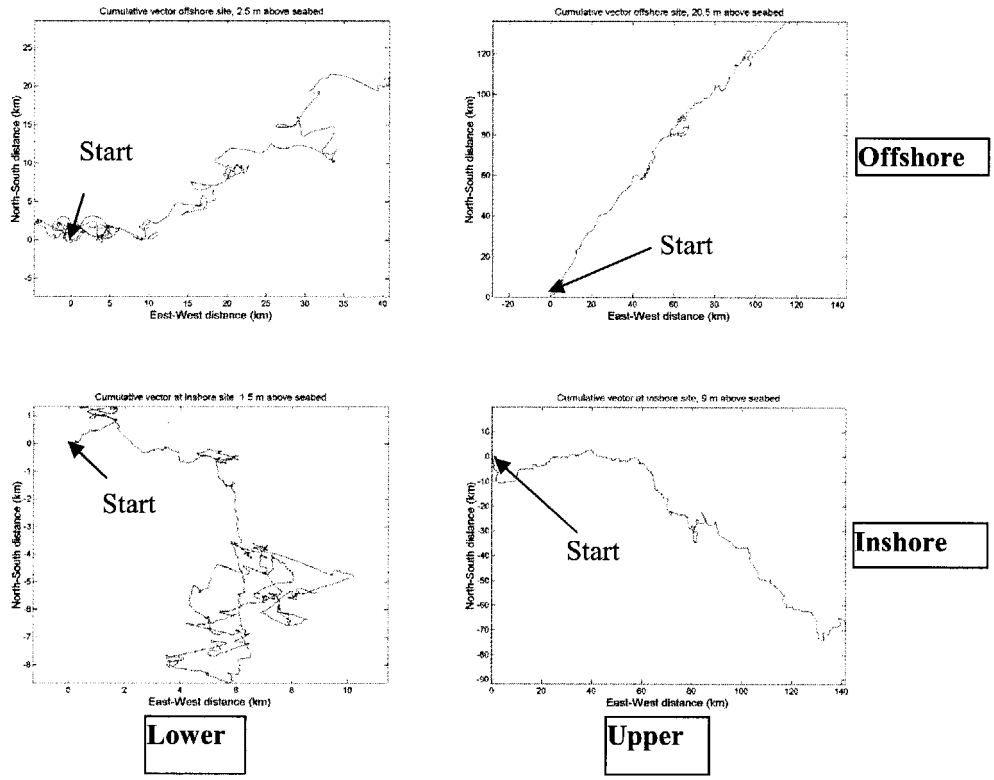

Figure 11: Cumulative vector plots at the offshore (upper) and inshore (lower) sites, in the upper (right) and lower (left) water column.

3.4 Stratification

Figure 12 shows that the water column was not strongly temperature stratified during the deployment (early spring season). Therefore three-dimensional effects such as up- and down-welling will be less likely, resulting in relatively uniform currents throughout the water column during the deployment. Stronger stratification could be expected during summer. The stratification over the deployment was dominated by diurnal surface temperature fluctuations (arising from daily solar heating and cooling), with a standard deviation of 0.40°C at 0.5 m decreasing to 0.15°C at 23.5 m. The maximum difference in the deployment-mean temperatures was between depths

0.08°C, and the mean temperature difference between 0.5 and 23 m depth was 0.04°C. These are consistent for coastal waters during spring when the water column is well mixed.

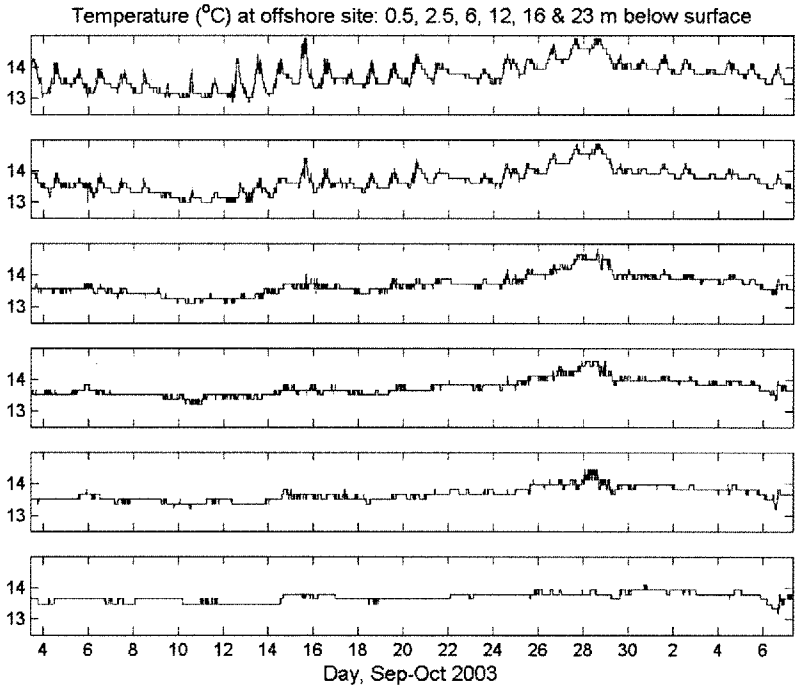

Figure 12: Temperature time-series measured at the offshore site (24 m water depth) by Tidbit loggers at approximately 0.5 (uppermost plot), 2.5, 6, 12, 16 and 23 m (lowermost plot) below the water surface.

3.5 Waves

Waves were measured in 20 minutes bursts every 3 hours. Wave statistics at the inshore site are shown in Figure 13. The mean significant wave height[1] (H_s) was 0.94 m and the maximum recorded wave height (H_{max}) was 3.1 m on 5th October during a southerly wind. Waves generally approached from the east through southeast quadrant (90-135°T) with periods of 5-12 seconds.

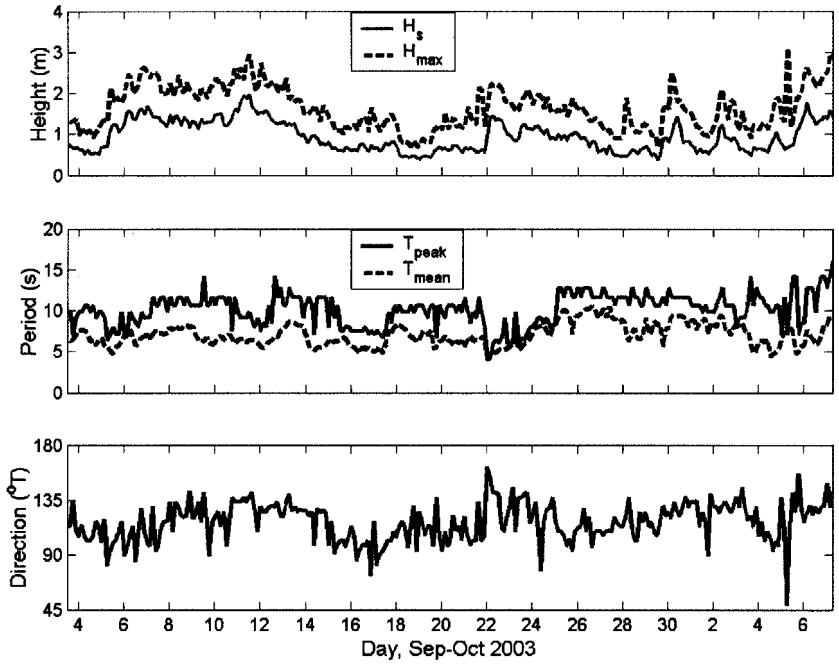

Figure 13: Three-hourly wave statistics from spectra measured at the inner site. H_s and H_{max} are significant and maximum wave height respectively, T_{peak} and T_{mean} are peak and mean wave period respectively, and the direction shown is peak direction of approach at the peak period.

[1] Significant wave height H, is the mean of the top 33% of wave heights during the 20 minute sampling period.

4. Summary

Currents, waves and water temperatures were measured in the Te Tapuwae O Rongokako Marine Reserve from 3 September to 7 October 2003, from deployments made at an offshore site in 24 m depth and an inshore site in 10 m depth.

At the offshore site mean current speeds ranged from 8 to 11 em s^{-1} and at the inshore site mean current speeds ranged from 4 to 10 cm s^{-1}. Tidal current speeds at the offshore site averaged 5.6 cm s^{-1}, and mainly flowed alongshore. Tidal currents were comparatively weak at the inshore site with mean speed of 2.8 cm s^{-1}. The tidal currents with largest amplitudes were the K_1 lunar-solar diurnal (once a day), the principal-lunar diurnal O_1 and the more well-known lunar semi-diurnal (twice-daily) M_2 tide.

A wavelet analysis showed that local winds were driving some of the non-tidal currents. The mean current direction through the marine reserve is alongshore to the northeast. This was measured at the offshore site and is supported by measurements made at other locations on this coast during four separate studies.

The water column was not strongly temperature stratified during the spring deployment, but stronger stratification could be expected during summer. The stratification over the deployment was dominated by diurnal surface temperature fluctuations (arising from daily solar heating and cooling), and the mean temperature difference between 0.5 and 23 m depth was 0.04°C.

The mean significant wave height during the deployment was 0.94 m and the maximum recorded wave height was 3.1 m on 5th October during a southerly wind. Waves generally approached from the east through southeast quadrant (90-135 °T) with periods of 5-12 seconds.

5. References

Bell, R.G. (1985). Coastal current data from Aanderaa current meter deployments 1982-1985. *DSIR Water Quality Centre, Hamilton, Internal Report 85/11.*

Chiswell, R.J.; Roemmich, D. (1998). The East Cape current and two eddies: a mechanism for larval retention. *New Zealand Journal of Marine and Freshwater Research 32(3)*: 385-397.

Chiswell, S.M. (2000). The Wairarapa Coastal Current. *New Zealand Journal of Marine and Freshwater Research 34(2)*: 303-315.

Heath, R.A. (1985). A review of the physical oceanography of the seas around New Zealand-1982. *New Zealand Journal of Marine and Freshwater Research 19:* 79-124.

Hessell, J.W.D. (1980). The climate and weather of the Gisborne region. *New Zealand meteorological service miscellaneous publication 115(8)*: 29.

Hsu, S.A. (1986). Correction of land-based wind data for offshore applications: A further evaluation. *Journal of Physical Oceanography 16(2)*: 390-394.

Laing, A.K.; Brenstrum, E. (1996). Scatterometer observations of low-level wind jets over New Zealand coastal waters. *Weather and Forecasting 11(4):* 458-475.

Pond, S.; Pickard, G.L. (1983). Introductory dynamical oceanography. 2. Pergamon Press, New York. 329 p.

Stephens, S.A.; Bell, R.G.; Black, K.P. (2001). Complex circulation in a coastal embayment: shelf current, wind and density-driven circulation in Poverty Bay, New Zealand. *Journal of Coastal Research Special Issue 34, ICS 2000 proceedings:* 45-59.

Torrence, C.; Compo, G.P. (1998). A practical guide to wavelet analysis. *Bulletin of the American Meteorological Society 79(1):* 61-78.

Walters, R.A.; Goring, D.G.; Bell, R.G. (2001). Ocean tides around New Zealand. *New Zealand Journal of Marine and Freshwater Research 35*: 567-579.